

First measurement of tau appearance with KM3NeT/ORCA6

Nicole Geißelbrecht^{a,*} for the KM3NeT collaboration

^a*Friedrich-Alexander-Universität Erlangen-Nürnberg (FAU), Erlangen Centre for Astroparticle Physics,
Nikolaus-Fiebiger-Straße 2, 91058 Erlangen, Germany*

E-mail: nicole.geisselbrecht@fau.de

KM3NeT/ORCA is an underwater Cherenkov neutrino detector currently being built in the Mediterranean Sea. The detector is optimised for the detection of atmospheric neutrinos in the energy range from a few GeV to 100 GeV in order to study neutrino oscillations and to determine the neutrino mass ordering.

The observation of oscillations of atmospheric electron and muon neutrinos into tau neutrinos is a primary physics goal during the ongoing detector construction phase, with a partially instrumented volume. The tau neutrino flux at the detector can be determined in a first step by identifying a statistical excess in the shower-like event topology compared to the expectation without oscillations. This measurement will allow to probe the standard three-flavour neutrino oscillation model.

This contribution will present the sensitivity of KM3NeT/ORCA to tau neutrino appearance and report a first measurement with ORCA6, an early 5% detector sub-array for an exposure of 433 kton-years.

38th International Cosmic Ray Conference (ICRC2023)
26 July - 3 August, 2023
Nagoya, Japan



*Speaker

1. Introduction - Tau appearance with KM3NeT/ORCA

The KM3NeT collaboration is currently building two neutrino telescopes in the Mediterranean Sea [1]. KM3NeT/ARCA is located near Sicily and is designed for neutrino astronomy. KM3NeT/ORCA is instead located offshore Toulon, France, and is optimised for the detection of atmospheric neutrinos in the energy range from a few to 100 GeV. The main goal is the study of neutrino oscillations and finally the determination of the neutrino mass ordering. Both detectors are three-dimensional arrays of photomultiplier tubes (PMTs) which detect the Cherenkov light that is emitted by the charged particles produced in neutrino interactions inside or close to the instrumented detector volume. KM3NeT/ORCA will consist of 115 vertical strings or detection units (DUs) anchored to the sea floor, and with an average distance of 20 metres. A DU comprises 18 so-called digital optical modules (DOMs) spaced 9 metres, and each DOM houses 31 3-inch PMTs in a 17-inch glass sphere. Data taking is already ongoing with preliminary sub-arrays of both detectors.

Sensitivity studies have shown that KM3NeT/ORCA has large potential for the observation of tau neutrinos [2]. The full detector will detect more than 3000 charged current tau neutrino (ν_τ CC) events per year. These tau neutrinos must be a product of neutrino oscillations (tau appearance) since the atmospheric neutrino flux below 100 GeV is initially almost entirely composed by electron and muon neutrinos from the decays of charged pions and kaons. The dominant production channel for tau neutrinos in KM3NeT/ORCA is the transition $\nu_\mu \rightarrow \nu_\tau$. Figure 1 shows the oscillation probability at the detector level, i.e. the bottom of the Sea, dependant on the neutrino energy and direction, where the most prominent oscillation maximum corresponds to vertically up-going neutrino events with energies between 20 and 30 GeV. Matter effects, leading to the discontinuity in the probability pattern, affect the transition probabilities mostly at lower energies and are not expected to have a sizeable impact on this analysis.

However, it is not possible to detect tau neutrinos in KM3NeT/ORCA on an event-by-event basis but only statistically since the event topology is too similar to other neutrino interactions. Charged current muon neutrino (ν_μ CC) interactions lead to a so-called track-like event signature in the detector. On the other hand, ν_τ CC interactions are mostly shower-like. As a consequence, tau appearance can be observed as a statistical excess of shower-like events.

Tau appearance is quantified through the so-called tau normalisation parameter, n_τ , which is defined as the ratio of the measured tau neutrino flux to the tau neutrino flux which is expected in the standard three-flavour neutrino oscillation scenario using the most updated measurements of the parameters that describe neutrino physics. There are non-negligible uncertainties on the charged current tau neutrino cross section [3] and on the unitarity of the PMNS matrix, especially in the tau sector [4], which could cause a deviation from the expected value. These two scenarios are respectively addressed by considering a scaling only on the CC component (CC-only), or by additionally scaling the expected fraction of neutral current (NC) events produced by tau neutrinos (CC+NC).

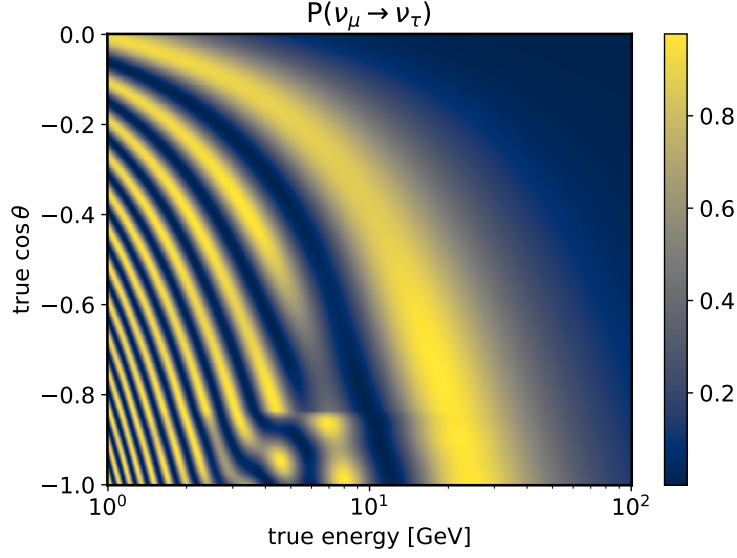


Figure 1: $\nu_\mu \rightarrow \nu_\tau$ oscillation probability at the detector level assuming normal ordering for true neutrino energy and direction relevant for KM3NeT/ORCA. Note that $\cos \theta$ equal to 0 (-1) refers to events that enter the detector horizontally (from below).

2. Data sample

This analysis is done with an early 5% sub-array of the full KM3NeT/ORCA detector composed of six detection units (KM3NeT/ORCA6). The total livetime is 510 days which corresponds to an exposure of 433 kton-years.

In order to obtain a clean neutrino sample, first, a pre-selection based on simple cuts which aims to discard pure noise events, is done. In a second step, atmospheric muon events are rejected by means of an event classifier based on boosted decision trees. Finally, the remaining events are further classified by a second set of boosted decision trees into track- and shower-like events. In order to minimise the impact of misclassified atmospheric muons and enhance the sensitivity, the track-like class is subdivided into a lower purity class (Low Purity Tracks) which contains the major amount of misclassified muons, and a higher purity class (High Purity Tracks) which contains only a very small fraction of muons.

The measurement of the tau normalisation parameter is carried out by fitting a model which includes the tau normalisation as a free parameter, to the observed event distribution in the two-dimensional space defined by the reconstructed energy and direction. To do this, histograms are created for each event class where the reconstructed direction is divided into 10 equally spaced bins in the up-going range of $\cos \theta$, where θ is the reconstructed zenith angle of an event. This is supposed to further reject the main background in KM3NeT/ORCA which is given by atmospheric muons that only enter the detector from above. Since tau neutrinos are only expected to come from below, this cut is not expected to have a negative impact on this analysis. Furthermore, 14 reconstructed energy bins are used between 2 and 100 GeV. In case of the shower class, one additional bin for events with reconstructed energies between 100 GeV and 1 TeV is introduced. After optimising the event

Oscillation parameter	Prior	Nuisance parameter	Prior
θ_{12}	fixed	Spectral Index	± 0.3
θ_{13}	fixed	$\nu_{\text{hor}}/\nu_{\text{ver}}$	$\pm 2\%$
θ_{23}	free	$\nu_{\mu}/\bar{\nu}_{\mu}$	$\pm 5\%$
Δm_{31}^2	free	$\nu_e/\bar{\nu}_e$	$\pm 7\%$
Δm_{21}^2	fixed	ν_{μ}/ν_e	$\pm 2\%$
δ_{CP}	fixed	NC Normalisation	$\pm 20\%$
		Energy scale	$\pm 9\%$
		High-energy Light Simulation	$\pm 50\%$
		Overall Normalisation	free
		Track Normalisation	free
		Shower Normalisation	free
		Muon Normalisation	free

Table 1: All systematic uncertainties and their treatment in the fit.

selection and classification as described above, about 200 ν_{τ} CC events are expected to be measured in 433 kton-years.

3. Measurement

3.1 Fit and systematic uncertainties

The tau normalisation is fitted by the minimisation of a negative log-likelihood function \mathcal{L} . The fit is performed in the two-dimensional plane of reconstructed energy and direction for all event type classes.

$$-2 \log \mathcal{L} = 2 \sum_{ij} \left(n_{ij}^{\text{model}} - n_{ij}^{\text{data}} + n_{ij}^{\text{model}} \log \left(\frac{n_{ij}^{\text{data}}}{n_{ij}^{\text{model}}} \right) \right) + \sum_{\epsilon} \left(\frac{\epsilon_{\text{exp}} - \epsilon_{\text{obs}}}{\sigma_{\epsilon}} \right)^2 \quad (1)$$

However, the fit does not only take n_{τ} into account but also the neutrino oscillation parameters, as well as other nuisance parameters as systematic uncertainties. The different parameters of the model as well as their treatment in the fit, i.e. if they are fitted with or without constraints, can be found in table 1. For each parameter ϵ with a prior σ_{ϵ} , a term is added to equation 1 which penalises fitted values outside the prior range. The fixed oscillation parameters are taken from NuFIT v5.0 (with SK atmospheric data) [5] with both mass orderings tested. The remaining nuisance parameters account for uncertainties in the atmospheric neutrino flux and cross section. The priors are taken from [6]. The energy scale is a single parameter that combines different uncertainties of the detector. The high-energy light simulation parameter addresses the different light generators that are used in the simulations for low- and high-energy neutrinos. Finally, the global normalisation (Overall Normalisation) and the normalisations concerning the Showers (Shower Normalisation), the High Purity Tracks (Track Normalisation) and the atmospheric muons (Muon Normalisation) are fitted without constraints.

3.2 Results

The tau appearance analysis has been performed for CC-only and CC+NC scaling. The tau normalisation and the corresponding 1σ uncertainty were found to be $0.50^{+0.46}_{-0.42}$ ($0.67^{+0.37}_{-0.33}$) for CC-only (CC+NC). The $\Delta \log \mathcal{L}$ profile is shown in figure 2. It presents the difference between the log-likelihoods of the best fit and models with a tau normalisation fixed to values between 0 and 2. Even though the measurement deviates from the expected value of 1, it is still consistent with $n_\tau = 1$ on a 1.1σ (0.9σ) level in case of CC-only (CC+NC). For CC+NC, no tau appearance, i.e., $n_\tau = 0$, is disfavoured with 2.2σ , whereas in the CC-only case, the measured value of n_τ agrees with no tau appearance within a 1.2σ level.

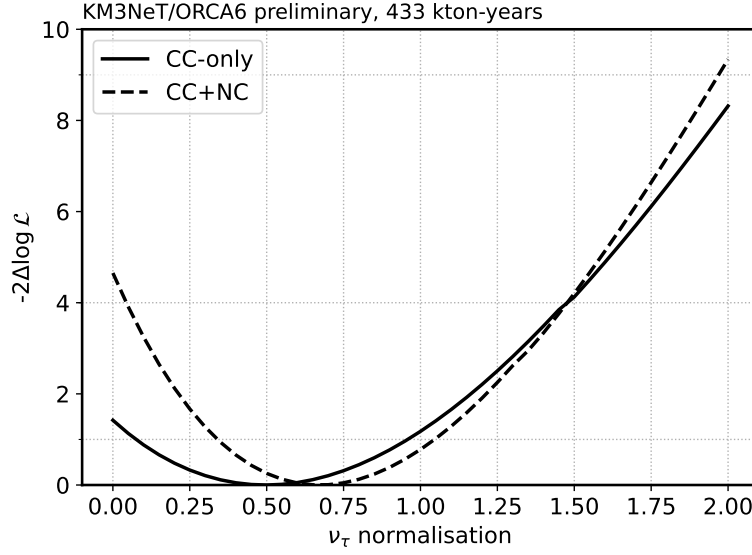


Figure 2: Measured $\Delta \log$ -likelihood profile for CC-only (solid) and CC+NC (dashed).

As presented in figure 1, the oscillation probability and hence tau appearance depends on L/E where L is the neutrino baseline which depends on $\cos \theta$ and E is the energy. Figure 3 shows the observed L/E distribution of shower-like events, compared to the best fit with respect to no tau appearance for CC-only and CC+NC, respectively. Additionally, the distribution for a model with $n_\tau = 1$ is shown.

Figure 4 shows the impacts and pulls of all fitted oscillation and nuisance parameters. In order to study the impact that a variation on a certain model parameter has on the fitted tau normalisation, two additional fits are performed where the parameter is fixed at its best fit \pm the 1σ MINOS errors calculated by the MINUIT package [7], while the rest of the parameters are left free. The impact on the tau normalisation is then calculated as $(n_\tau^{\text{shift}} - n_\tau^{\text{bf}}) / \sigma_{n_\tau}$. The coloured bars on figure 4 summarise the impact of the different parameters on the tau normalisation. For both scalings, the normalisation factors for the different light generators and the shower class as well as the zenith slope have large impacts. Slight differences between CC-only and CC+NC are a result of different correlations between the respective tau normalisation and the systematic uncertainties.

The black markers and their associated error bars on figure 4 represent the so-called pulls, which are

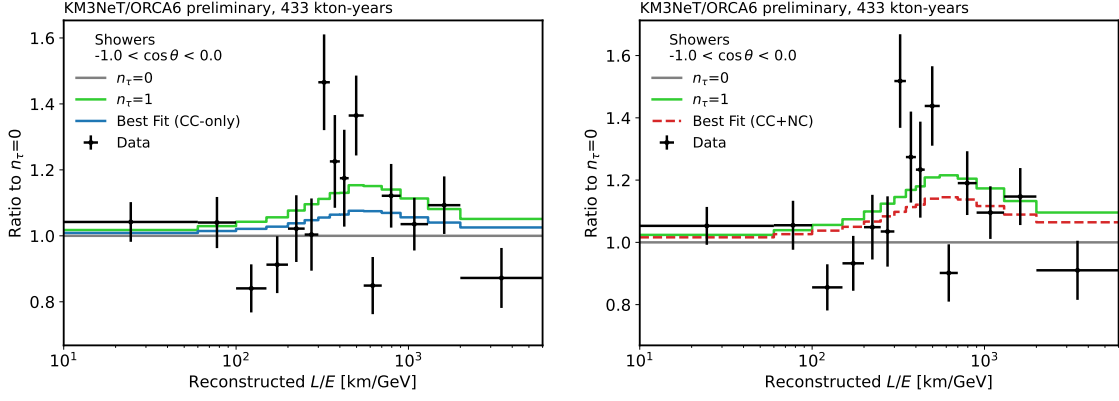


Figure 3: L/E distributions for data, the best fit and $n_{\tau} = 1$ of the shower class with respect to no tau appearance for CC-only (left) and CC+NC (right).

defined as the difference of the best fit value and the expected value with respect to its uncertainty $(\epsilon_{\text{BF}} - \epsilon_{\text{CV}}) / \sigma$. Here, σ represents the pre-fit uncertainty in the parameter whenever available. For those parameters without pre-fit uncertainty, σ represents the post-fit uncertainty. The error bars are calculated as the ratio $\sigma_{\epsilon}^{\text{post-fit}} / \sigma_{\epsilon}^{\text{pre-fit}}$ or set to 1 for those parameters without pre-fit uncertainties. As can be seen, the systematics with the largest pulls are the normalisations and the oscillation parameters. This can be expected since these are the parameters that are fitted without prior.

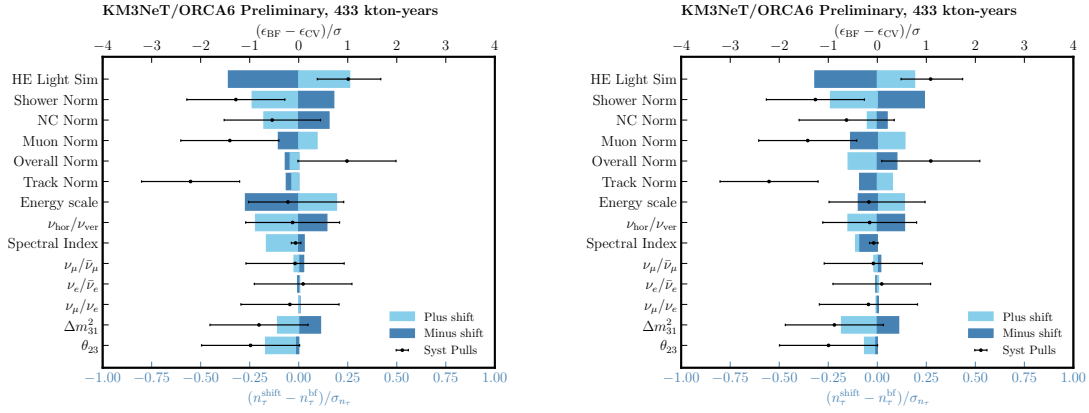


Figure 4: Impact on the tau normalisation of fixing oscillation and nuisance parameters at their best fit value $\pm 1\sigma$ (post-fit) uncertainty with respect to its uncertainty (coloured bars, lower axis). Additionally, the pulls and constraints (black markers with error bars, upper axis) are shown. Left: CC-only. Right: CC+NC.

Figure 5 presents the comparison of the results of KM3NeT/ORCA6 with the measurements of the tau normalisation that have been performed so far by OPERA [9], Super-Kamiokande [10] and IceCube/DeepCore [8]. All measurements agree with the Standard Model within their reported uncertainties. The first two experiments observed a tau normalisation larger than expected. However, a direct comparison of the results is non-trivial: on one hand, the differences with respect to OPERA could be related to the different neutrino sources used by both experiments. On the other hand, Super-Kamiokande's measurement was performed in an energy range where deep inelastic scattering

contributes a 41% to the neutrino cross section, while being the main interaction channel in the KM3NeT/ORCA measurement. A direct comparison to the results of IceCube/DeepCore would be more straightforward because both detectors use the same neutrino source and both measurements are conducted in the same energy range. The measured tau normalisations from KM3NeT/ORCA6 and IceCube/DeepCore agree within a 1σ level. As can be seen in figure 5, none of the so far performed measurements can rule out a tau normalisation equal to 1.

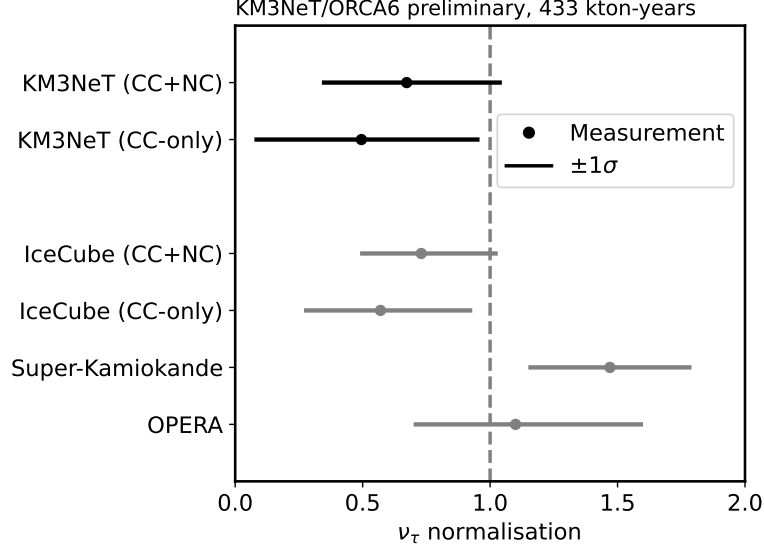


Figure 5: Comparison of the results for the tau normalisation from the different experiments. The errorbars show the reported 1σ uncertainties. Results are taken from [9] (OPERA), [10] (Super-Kamiokande) and [8] (IceCube/DeepCore).

4. Conclusion and Outlook

The first measurement of the tau normalisation for KM3NeT/ORCA6 has been performed for a data set with an exposure of 433 kton-years. The results are consistent with the expectations of a tau normalisation equal to 1, even though they indicate a slightly lower value than expected, namely $n_\tau = 0.50^{+0.46}_{-0.42}$ ($0.67^{+0.37}_{-0.33}$) for CC-only (CC+NC). The uncertainties of this measurement are on the same order of magnitude as the previous measurements from other experiments. However, the uncertainty is expected to be reduced in the future with extended data sets and larger detector configurations. This will decrease the impact of the statistical as well as of the systematic uncertainties. For an exposure of 21 Mton-years, which corresponds to 3 years of data taking with the full KM3NeT/ORCA detector, the tau normalisation will be constrained to $\pm 7\%$ on a 1σ level (CC-only) [2]. On the long term, the measurement of n_τ can help to constrain elements of the PMNS matrix, as well as to constrain the ν_τ CC deep inelastic scattering cross section.

References

- [1] S. Adrián-Martínez, et al. "Letter of intent for KM3NeT 2.0". In: *Journal of Physics G: Nuclear and Particle Physics* 43.8 (2016), p. 084001. DOI: 10.1088/0954-3899/43/8/084001. URL: <https://doi.org/10.1088%2F0954-3899%2F43%2F8%2F084001>.
- [2] S. Aiello, M. Ageron, et al. "Determining the neutrino mass ordering and oscillation parameters with KM3NeT/ORCA". In: *The European Physical Journal C* 82.1 (2022). DOI: 10.1140/epjc/s10052-021-09893-0. URL: <https://doi.org/10.1140%2Fepjc%2Fs10052-021-09893-0>.
- [3] Y. S. Jeong and M. H. Reno. "Tau neutrino and antineutrino cross sections". In: *Physical Review D* 82.3 (2010). DOI: 10.1103/physrevd.82.033010. URL: <https://doi.org/10.1103%2Fphysrevd.82.033010>.
- [4] S. Parke and M. Ross-Lonergan. "Unitarity and the three flavor neutrino mixing matrix". In: *Phys. Rev. D* 93 (11 2016), p. 113009. DOI: 10.1103/PhysRevD.93.113009. URL: <https://link.aps.org/doi/10.1103/PhysRevD.93.113009>.
- [5] I. Esteban, M. Gonzalez-Garcia, et al. "The fate of hints: updated global analysis of three-flavor neutrino oscillations". In: *Journal of High Energy Physics* 2020.9 (2020). DOI: 10.1007/jhep09(2020)178. URL: <https://doi.org/10.1007%2Fjhep09%282020%29178>.
- [6] G. D. Barr, S. Robbins, et al. "Uncertainties in atmospheric neutrino fluxes". In: *Physical Review D* 74.9 (2006). DOI: 10.1103/physrevd.74.094009. URL: <https://doi.org/10.1103%2Fphysrevd.74.094009>.
- [7] F. James. *MINUIT: function minimization and error analysis reference manual*. Tech. rep. Cern, 1998.
- [8] M. Aartsen, M. Ackermann, et al. "Measurement of atmospheric tau neutrino appearance with IceCube DeepCore". In: *Physical Review D* 99.3 (2019). DOI: 10.1103/physrevd.99.032007. URL: <https://doi.org/10.1103%2Fphysrevd.99.032007>.
- [9] N. Agafonova, A. Alexandrov, et al. "Final Results of the OPERA Experiment on ν_τ Appearance in the CNGS Neutrino Beam". In: *Phys. Rev. Lett.* 120 (21 2018), p. 211801. DOI:10.1103/PhysRevLett.120.211801. URL: <https://link.aps.org/doi/10.1103/PhysRevLett.120.211801>.
- [10] Z. Li, K. Abe, et al. "Measurement of the tau neutrino cross section in atmospheric neutrino oscillations with Super-Kamiokande". In: *Physical Review D* 98.5 (2018). DOI: 10.1103/physrevd.98.052006. URL: <https://doi.org/10.1103%2Fphysrevd.98.052006>.

Full Authors List: The KM3NeT Collaboration

S. Aiello^a, A. Albert^{b,bed}, S. Alves Garre^c, Z. Aly^d, A. Ambrosone^{f,e}, F. Ameli^g, M. Andre^h, E. Androutsouⁱ, M. Anguita^j, L. Aphecetche^k, M. Ardid^l, S. Ardid^l, H. Atmani^m, J. Aublinⁿ, L. Bailly-Salins^o, Z. Bardáčová^{q,p}, B. Baretⁿ, A. Bariego-Quintana^c, S. Basegmez du Pree^r, Y. Becheriniⁿ, M. Bendahman^{m,n}, F. Benfenati^{t,s}, M. Benhassi^{u,e}, D. M. Benoit^v, E. Berbee^r, V. Bertin^d, S. Biagi^w, M. Boettcher^x, D. Bonanno^w, J. Boumaaza^m, M. Bouta^y, M. Bouwhuis^r, C. Bozza^{z,e}, R. M. Bozza^{f,e}, H. Brânzaş^{aa}, F. Bretaudeau^k, R. Bruijn^{ab,r}, J. Brunner^d, R. Bruno^a, E. Buis^{ac,r}, R. Buompane^{u,e}, J. Busto^d, B. Caiffi^{ad}, D. Calvo^c, S. Champion^{g,ae}, A. Capone^{g,ae}, F. Carenini^{t,s}, V. Carretero^c, T. Cartraudⁿ, P. Castaldi^{af,s}, V. Cecchini^c, S. Celli^{g,ae}, L. Cerisy^d, M. Chabab^{ag}, M. Chadolias^{ah}, A. Chen^{ai}, S. Cherubini^{aj,w}, T. Chiarusi^s, M. Circella^{ak}, R. Cocimano^w, J. A. B. Coelhoⁿ, A. Coleiroⁿ, R. Coniglione^w, P. Coyle^d, A. Creusotⁿ, A. Cruz^{al}, G. Cuttone^w, R. Dallier^k, Y. Darras^{ah}, A. De Benedittis^e, B. De Martino^d, V. Decoene^k, R. Del Burgo^e, U. M. Di Cerbo^e, L. S. Di Mauro^w, I. Di Palma^{g,ae}, A. F. Díaz^j, C. Díaz^j, D. Diego-Tortosa^w, C. Distefano^w, A. Domi^{ah}, C. Donzau^d, D. Dornic^d, M. Dörr^{am}, E. Drakopoulouⁱ, D. Drouhin^{b,bd}, R. Dvornický^q, T. Eberl^{ah}, E. Eckerová^{q,p}, A. Eddymaoui^m, T. van Eeden^r, M. Effⁿ, D. van Eijk^r, I. El Bojaddaini^y, S. El Hedriⁿ, A. Enzenhöfer^d, G. Ferrara^w, M. D. Filipović^{an}, F. Filippini^{t,s}, D. Franciotti^w, L. A. Fusco^{z,e}, J. Gabriel^{ao}, S. Gagliardini^g, T. Gal^{ah}, J. García Méndez^l, A. Garcia Soto^c, C. Gatiu Oliver^r, N. Geißelbrecht^{ah}, H. Ghaddari^y, L. Gialanella^u, B. K. Gibson^v, E. Giorgio^w, I. Goosⁿ, D. Goupilliere^o, S. R. Gozzini^c, R. Gracia^{ah}, K. Graf^{ah}, C. Guidi^{ap,ad}, B. Guillon^o, M. Gutiérrez^{aq}, H. van Haren^{ar}, A. Heijboer^r, A. Hekalo^{am}, L. Hennig^{ah}, J. J. Hernández-Rey^c, F. Huang^d, W. Idrissi Ibsalih^e, G. Illuminati^s, C. W. James^{al}, M. de Jong^{as,r}, P. de Jong^{ab,r}, B. J. Jung^r, P. Kalaczynski^{ai,be}, O. Kalekin^{ah}, U. F. Katz^{ah}, N. R. Khan Chowdhury^c, A. Khatun^q, G. Kistauri^{av,au}, C. Kopper^{ah}, A. Kouchner^{aw,n}, V. Kulikovskiy^{ad}, R. Kvatadze^{av}, M. Labalme^o, R. Lahmann^{ah}, G. Larosa^w, C. Lasteria^d, A. Lazo^c, S. Le Stum^d, G. Lehaut^o, E. Leonora^a, N. Lessing^c, G. Levi^{t,s}, M. Lindsey Clarkⁿ, F. Longhitano^q, J. Majumdar^r, L. Malerba^{ad}, F. Mamedov^p, J. Mańczak^c, A. Manfreda^e, M. Marconi^{ap,ad}, A. Margiotta^{t,s}, A. Marinelli^{e,f}, C. Markouⁱ, L. Martin^k, J. A. Martínez-Mora^l, F. Marzaioli^{u,e}, M. Mastrodicasa^{ae,g}, S. Mastroianni^e, S. Micciché^w, G. Miele^{f,e}, P. Migliozzi^e, E. Migneco^w, M. L. Mitsou^e, C. M. Mollo^e, L. Morales-Gallegos^{u,e}, C. Morley-Wong^{al}, A. Moussa^y, I. Mozun Mateo^{ay,ax}, R. Müller^r, M. R. Musone^{e,u}, M. Musumeci^w, L. Nauta^r, S. Navas^{aq}, A. Nayerhoda^{ak}, C. A. Nicolau^g, B. Nkosi^{ai}, B. Ó Fearraigh^{ab,r}, V. Oliviero^{f,e}, A. Orlando^w, E. Oukacha^u, D. Paesani^w, J. Palacios González^c, G. Papalashvili^{au}, V. Parisi^{ap,ad}, E. J. Pastor Gomez^c, A. M. Păun^{aa}, G. E. Pávlaš^{aa}, S. Peña Martínezⁿ, M. Perrin-Terrin^d, J. Perronnel^o, V. Pestel^{ay}, R. Pestesⁿ, P. Piattelli^w, C. Poirè^{z,e}, V. Popa^{aa}, T. Pradier^b, S. Pulvirenti^w, G. Quémener^o, C. Quiroz^l, U. Rahaman^c, N. Randazzo^{aa}, R. Randriatoamanana^k, S. Razzaque^{az}, I. C. Rea^e, D. Real^c, S. Reck^{ah}, G. Riccobene^w, J. Robinson^x, A. Romanov^{ap,ad}, A. Šaina^c, F. Salsesa Greus^c, D. F. E. Samtleben^{as,r}, A. Sánchez Losa^{c,ak}, S. Sanfilippo^w, M. Sanguineti^{ap,ad}, C. Santonastaso^{ba,e}, D. Santonocito^w, P. Sapienza^w, J. Schnabel^{ah}, J. Schumann^{ah}, H. M. Schutte^x, J. Seneca^r, N. Sennan^y, B. Setter^{ah}, I. Sgura^{ak}, R. Shanidze^{au}, Y. Shitov^p, F. Šimković^q, A. Simonelli^e, A. Sinopoulou^a, M. V. Smirnov^{ah}, B. Spisso^e, M. Spurio^{t,s}, D. Stavropoulosⁱ, I. Štekl^p, M. Taiuti^{ap,ad}, Y. Tayalati^m, H. Tadjiti^{ad}, H. Thiersen^x, I. Tosta e Melo^{aj}, B. Trocméⁿ, V. Tsoarapisⁱ, E. Tzamaridou^{ki}, A. Vacheret^o, V. Valsecchi^w, V. Van Elewyck^{aw,n}, G. Vannoye^d, G. Vasileiadis^{bb}, F. Vazquez de Sola^r, C. Verilhac^u, A. Veutro^{g,ae}, S. Viola^w, D. Vivolo^{u,e}, J. Wilms^{bc}, E. de Wolf^{ab,r}, H. Yepes-Ramirez^l, G. Zarpapisiⁱ, S. Zavatarelli^{ad}, A. Zegarelli^{g,ae}, D. Zito^w, J. D. Zornoza^c, J. Zúñiga^c, and N. Zywucka^x.

^aINFN, Sezione di Catania, Via Santa Sofia 64, Catania, 95123 Italy

^bUniversité de Strasbourg, CNRS, IPHC UMR 7178, F-67000 Strasbourg, France

^cIFIC - Instituto de Física Corpuscular (CSIC - Universitat de València), c/Catedrático José Beltrán, 2, 46980 Paterna, Valencia, Spain

^dAix Marseille Univ, CNRS/IN2P3, CPPM, Marseille, France

^eINFN, Sezione di Napoli, Complesso Universitario di Monte S. Angelo, Via Cintia ed. G, Napoli, 80126 Italy

^fUniversità di Napoli "Federico II", Dip. Scienze Fisiche "E. Pancini", Complesso Universitario di Monte S. Angelo, Via Cintia ed. G, Napoli, 80126 Italy

^gINFN, Sezione di Roma, Piazzale Aldo Moro 2, Roma, 00185 Italy

^hUniversitat Politècnica de Catalunya, Laboratori d'Aplicacions Bioacústiques, Centre Tecnològic de Vilanova i la Geltrú, Avda. Rambla Exposició, s/n, Vilanova i la Geltrú, 08800 Spain

ⁱNCSR Demokritos, Institute of Nuclear and Particle Physics, Ag. Paraskevi Attikis, Athens, 15310 Greece

^jUniversity of Granada, Dept. of Computer Architecture and Technology/CITIC, 18071 Granada, Spain

^kSubatech, IMT Atlantique, IN2P3-CNRS, Université de Nantes, 4 rue Alfred Kastler - La Chantrerie, Nantes, BP 20722 44307 France

^lUniversitat Politècnica de València, Instituto de Investigación para la Gestión Integrada de las Zonas Costeras, C/Paranimf, 1, Gandia, 46730 Spain

^mUniversity Mohammed V in Rabat, Faculty of Sciences, 4 av. Ibn Battouta, B.P. 1014, R.P. 10000 Rabat, Morocco

ⁿUniversité Paris Cité, CNRS, Astroparticule et Cosmologie, F-75013 Paris, France

^oLPC CAEN, Normandie Univ, ENSICAEN, UNICAEN, CNRS/IN2P3, 6 boulevard Maréchal Juin, Caen, 14050 France

^pCzech Technical University in Prague, Institute of Experimental and Applied Physics, Husova 240/5, Prague, 110 00 Czech Republic

^qComenius University in Bratislava, Department of Nuclear Physics and Biophysics, Mlynska dolina F1, Bratislava, 842 48 Slovak Republic

^rNikhef, National Institute for Subatomic Physics, PO Box 41882, Amsterdam, 1009 DB Netherlands

^sINFN, Sezione di Bologna, v.le C. Berti-Pichat, 6/2, Bologna, 40127 Italy

^tUniversità di Bologna, Dipartimento di Fisica e Astronomia, v.le C. Berti-Pichat, 6/2, Bologna, 40127 Italy

^uUniversità degli Studi della Campania "Luigi Vanvitelli", Dipartimento di Matematica e Fisica, viale Lincoln 5, Caserta, 81100 Italy

^vE. A. Milne Centre for Astrophysics, University of Hull, Hull, HU6 7RX, United Kingdom

- ^wINFN, Laboratori Nazionali del Sud, Via S. Sofia 62, Catania, 95123 Italy
- ^xNorth-West University, Centre for Space Research, Private Bag X6001, Potchefstroom, 2520 South Africa
- ^yUniversity Mohammed I, Faculty of Sciences, BV Mohammed VI, B.P. 717, R.P. 60000 Oujda, Morocco
- ^zUniversità di Salerno e INFN Gruppo Collegato di Salerno, Dipartimento di Fisica, Via Giovanni Paolo II 132, Fisciano, 84084 Italy
- ^{aa}ISS, Atomistilor 409, Măgurele, RO-077125 Romania
- ^{ab}University of Amsterdam, Institute of Physics/IHEF, PO Box 94216, Amsterdam, 1090 GE Netherlands
- ^{ac}TNO, Technical Sciences, PO Box 155, Delft, 2600 AD Netherlands
- ^{ad}INFN, Sezione di Genova, Via Dodecaneso 33, Genova, 16146 Italy
- ^{ae}Università La Sapienza, Dipartimento di Fisica, Piazzale Aldo Moro 2, Roma, 00185 Italy
- ^{af}Università di Bologna, Dipartimento di Ingegneria dell'Energia Elettrica e dell'Informazione "Guglielmo Marconi", Via dell'Università 50, Cesena, 47521 Italia
- ^{ag}Cadi Ayyad University, Physics Department, Faculty of Science Semlalia, Av. My Abdellah, P.O.B. 2390, Marrakech, 40000 Morocco
- ^{ah}Friedrich-Alexander-Universität Erlangen-Nürnberg (FAU), Erlangen Centre for Astroparticle Physics, Nikolaus-Fiebiger-Straße 2, 91058 Erlangen, Germany
- ^{ai}University of the Witwatersrand, School of Physics, Private Bag 3, Johannesburg, Wits 2050 South Africa
- ^{aj}Università di Catania, Dipartimento di Fisica e Astronomia "Ettore Majorana", Via Santa Sofia 64, Catania, 95123 Italy
- ^{ak}INFN, Sezione di Bari, via Orabona, 4, Bari, 70125 Italy
- ^{al}International Centre for Radio Astronomy Research, Curtin University, Bentley, WA 6102, Australia
- ^{am}University Würzburg, Emil-Fischer-Straße 31, Würzburg, 97074 Germany
- ^{an}Western Sydney University, School of Computing, Engineering and Mathematics, Locked Bag 1797, Penrith, NSW 2751 Australia
- ^{ao}IN2P3, LPC, Campus des Cégeaux 24, avenue des Landais BP 80026, Aubière Cedex, 63171 France
- ^{ap}Università di Genova, Via Dodecaneso 33, Genova, 16146 Italy
- ^{aq}University of Granada, Dpto. de Física Teórica y del Cosmos & C.A.F.P.E., 18071 Granada, Spain
- ^{ar}NIOZ (Royal Netherlands Institute for Sea Research), PO Box 59, Den Burg, Texel, 1790 AB, the Netherlands
- ^{as}Leiden University, Leiden Institute of Physics, PO Box 9504, Leiden, 2300 RA Netherlands
- ^{at}National Centre for Nuclear Research, 02-093 Warsaw, Poland
- ^{au}Tbilisi State University, Department of Physics, 3, Chavchavadze Ave., Tbilisi, 0179 Georgia
- ^{av}The University of Georgia, Institute of Physics, Kostava str. 77, Tbilisi, 0171 Georgia
- ^{aw}Institut Universitaire de France, 1 rue Descartes, Paris, 75005 France
- ^{ax}IN2P3, 3, Rue Michel-Ange, Paris 16, 75794 France
- ^{ay}LPC, Campus des Cégeaux 24, avenue des Landais BP 80026, Aubière Cedex, 63171 France
- ^{az}University of Johannesburg, Department Physics, PO Box 524, Auckland Park, 2006 South Africa
- ^{ba}Università degli Studi della Campania "Luigi Vanvitelli", CAPACITY, Laboratorio CIRCE - Dip. Di Matematica e Fisica - Viale Carlo III di Borbone 153, San Nicola La Strada, 81020 Italy
- ^{bb}Laboratoire Univers et Particules de Montpellier, Place Eugène Bataillon - CC 72, Montpellier Cédex 05, 34095 France
- ^{bc}Friedrich-Alexander-Universität Erlangen-Nürnberg (FAU), Remeis Sternwarte, Sternwartstraße 7, 96049 Bamberg, Germany
- ^{bd}Université de Haute Alsace, rue des Frères Lumière, 68093 Mulhouse Cedex, France
- ^{be}AstroCeNT, Nicolaus Copernicus Astronomical Center, Polish Academy of Sciences, Rektorska 4, Warsaw, 00-614 Poland

Acknowledgements

The authors acknowledge the financial support of the funding agencies: Agence Nationale de la Recherche (contract ANR-15-CE31-0020), Centre National de la Recherche Scientifique (CNRS), Commission Européenne (FEDER fund and Marie Curie Program), LabEx UnivEarthS (ANR-10-LABX-0023 and ANR-18-IDEX-0001), Paris Île-de-France Region, France; Shota Rustaveli National Science Foundation of Georgia (SRNSFG, FR-22-13708), Georgia; The General Secretariat of Research and Innovation (GSRI), Greece Istituto Nazionale di Fisica Nucleare (INFN), Ministero dell'Università e della Ricerca (MIUR), PRIN 2017 program (Grant NAT-NET 2017W4HA7S) Italy; Ministry of Higher Education, Scientific Research and Innovation, Morocco, and the Arab Fund for Economic and Social Development, Kuwait; Nederlandse organisatie voor Wetenschappelijk Onderzoek (NWO), the Netherlands; The National Science Centre, Poland (2021/41/N/ST2/01177); The grant "AstroCeNT: Particle Astrophysics Science and Technology Centre", carried out within the International Research Agendas programme of the Foundation for Polish Science financed by the European Union under the European Regional Development Fund; National Authority for Scientific Research (ANCS), Romania; Grants PID2021-124591NB-C41, -C42, -C43 funded by MCIN/AEI/ 10.13039/501100011033 and, as appropriate, by "ERDF A way of making Europe", by the "European Union" or by the "European Union NextGenerationEU/PRTR", Programa de Planes Complementarios I+D+I (refs. ASFAE/2022/023, ASFAE/2022/014), Programa Prometeo (PROMETEO/2020/019) and GenT (refs. CIDEAGENT/2018/034, /2019/043, /2020/049, /2021/23) of the Generalitat Valenciana, Junta de Andalucía (ref. SOMM17/6104/UGR, P18-FR-5057), EU: MSC program (ref. 101025085), Programa María Zambrano (Spanish Ministry of Universities, funded by the European Union, NextGenerationEU), Spain; The European Union's Horizon 2020 Research and Innovation Programme (ChETEC-INFRA - Project no. 101008324).